N95-27642

ANALYSIS OF SELECTED SPECIMENS FROM THE STS-46 ENERGETIC OXYGEN INTERACTION WITH MATERIALS-III EXPERIMENT

Johnny L. Golden, Roger J. Bourassa, Harry W. Dursch and H. Gary Pippin

Boeing Defense & Space Group
P.O. Box 3999 M/S 82-32
Seattle, WA 98124-2499
(206) 773-2846, FAX (206) 773-4946

INTRODUCTION

The Energetic Oxygen Interaction with Materials III (EOIM-III) experiment was flown on the STS-46 mission, which was launched on July 31, 1992 and returned August 8, 1992. Boeing specimens were located on both the NASA Marshall Space Flight Center (MSFC) tray and the Ballistic Missile Defense Organization (BMDO) tray integrated by the Jet Propulsion Laboratory (JPL). The EOIM-III pallet was mounted in the Space Shuttle payload bay near the aft bulkhead.

During the mission, the atomic oxygen (AO) exposure levels of specimens in these passive sample trays was about 2.3×10^{20} atoms/cm^2. The specimens also received an estimated 22 equivalent sun hours of solar exposure (ref. 1). In addition, it appears that the EOIM-3 pallet was exposed to a silicone contamination source and many specimens had a thin layer of silicon based deposit on their surfaces after the flight (ref. 2).

The specimens on the MSFC tray included seven solid film lubricants, a selection of butyl rubber (B612) and silicone (S383) o-rings, three indirect scatter surfaces, and Silver/ Fluorinated Ethylene Propylene (Ag/FEP) and Chemglaze A276 specimens which had previously flown on trailing edge locations of the Long Duration Exposure Facility (LDEF). The specimens on the JPL tray included composites previously flown on LDEF and two indirect scattering surfaces. The indirect scattering surface specimens from both trays provided minimal information and will not be discussed in this paper. The o-ring specimens were exposed to the low Earth orbit (LEO) environment under a variety of selected tensile or compressive load conditions. The Chemglaze A276 polyurethane paint specimens from the LDEF had all been previously exposed to several thousand equivalent sun hours (ESH) of solar radiation during the LDEF flight. Selected composite and Ag/FEP specimens were also chosen because of their prior solar exposure. Additional composite and Ag/FEP specimens from the LDEF which had not been directly exposed to high solar fluences were also chosen for reflight. The intent of the environmental exposure for the composite and Ag/FEP specimens was to see if the prior solar exposure enhanced their recession rates when subsequently exposed to atomic oxygen.

RESULTS & ANALYSIS

Solid Film Lubricants

The eight solid film lubricants selected for test are shown in table 1. Weight measurements were made before and after flight under tightly controlled environmental conditions by NASA MSFC. Weight change results are also shown in table 1.

Table 1. Solid Film Lubricants and Their Weight Changes After The EOIM-III Flight.

NAME	DESCRIPTION	WEIGHT CHANGE
Tiolube 29	Inorganic Coating	<0.03 mg/cm^2
Tiolube 460	MoS_2 filled Organic Coating	-0.10 mg/cm^2
PS212	Chromium Carbide/Ag/Fluoride Eutectic Self-Lubricating Composite Coating	<0.03 mg/cm^2
Torlon 4301	Poly(amide-imide) Wear Resistant Polymer	+6.76 mg/cm^2
Delrin 100AF	PTFE filled Acetal Resin	-1.64 mg/cm^2
NPI 425	MoS_2/Sb oxide filled Polyimide Coating	-0.10 mg/cm^2
Garlock DU	PTFE/Pb filled with Tin Bronze	<0.03 mg/cm^2
Vitro-Lube (NPI 1220)	Ceramic Bonded MoS_2/Graphite/Ag With MoS_2/Graphite Phenolic Topcoat	-0.10 mg/cm^2

The outer ring of each lubricant specimen was covered by the lip of the aluminum sample holder. This provides unexposed material on each specimen to compare with the space exposed surface. Visual examination of the lubricants closely followed the weight change results. The two specimens with the significant weight changes both darkened with environmental exposure, as is shown in figure 1 for Torlon 4301 and in figure 2 for Delrin 100AF. For comparison, the appearance of PS212 changed very little (see figure 3).

Surface profilometry was used in an attempt to measure surface erosion at the exposed to unexposed interface on the flight specimens. Erosion was undetectable by this method.

X-ray photoelectron spectroscopy (XPS) was used to characterize the surfaces of all lubricants before and after exposure on EOIM-III. Samples of the information obtained are shown in figures 4 - 9. Comparison of the Garlock DU control specimen in figure 4 with the flight specimen (which indicated minimal weight change) in figure 5 shows that the lead (Pb) signals have increased significantly, presumably due to some erosion of the PTFE fraction. For the Tiolube 460 lubricant (which exhibited a slight weight change with exposure), comparison of the control specimen measurement in figure 6 to the flight specimen in figure 7 indicates that there has been a significant loss of carbon signal because of atomic oxygen erosion. Based on the spectrum of figure 7, the Tiolube 460

material also contains lead (Pb) and antimony (Sb). One final comparison involves the lubricant Torlon 4301, which gained significant weight with exposure on EOIM-III. Comparison of the control specimen in figure 8 with the flight specimen in figure 9 indicates a reduction in the carbon 1s signal for the flight specimen, but with no corresponding signal increases (such as for oxygen) to explain the weight increase observed for this material.

O-Rings

Fifteen specimens of butyl and silicone rubbers were flown as part of our investigation on EOIM-III. The specimens were exposed to the LEO space environment while subjected to various levels of tensile or compressive loading. Examples of the two tensile load specimen holders, as well as the compressive loading specimen holders, are shown mounted in the experiment tray (preflight) in figure 10. Stainless steel mesh covers the specimens in the tensile loading fixtures to ensure that the o-rings stayed with the experiment through sample recovery.

Scanning electron microscopy (SEM) images of the o-ring surfaces were made postflight. Figures 11 and 12 show comparison of the surfaces of butyl and silicone rubber o-rings that were held under compression during environmental exposure at 1000X and 3000X, respectively. General AO erosion is visible on the butyl rubber surfaces while no apparent erosion occurred on the silicone rubber. The silicone rubber was similarly unaffected in the tensile loading configuration. The butyl rubber, however, showed erosion patterns affected by the amount of tension applied. Figure 13 shows two butyl o-rings at 500X, the first loaded in tension by stretching it to 60% above its original diameter, the second to 100% above its original diameter. The 100% tension specimen has developed a cracking erosion pattern perpendicular to the direction of stress. Figure 14 shows a comparable erosion pattern at 80% tension. Also shown in figure 14 is the pattern of uneroded surface resulting from the AO shielding provided by the stainless steel mesh covers.

Visual examination of the two o-ring materials confirmed the erosion of butyl rubber surfaces because of the apparent loss of surface gloss. No visible effect was noted for silicone rubber o-rings. However, examination of the silicone rubber under ultraviolet illumination, as shown in figure 15, indicated that some chemical change, as evidenced by fluorescence, had occurred on the silicone surface with environmental exposure.

Graphite/Epoxy Composite

Two specimens of T300/934 graphite/epoxy composite that had previously flown on the Long Duration Exposure Facility (LDEF) were chosen for reflight on EOIM-III. The specimens were from LDEF experiment M0003-10. One of the specimens, 5C1A, had been exposed to 10,500 equivalent sun hours (ESH) of solar exposure and 2.3×10^5 atomic oxygen atoms/cm^2 during the LDEF mission. The other specimen, 5C2A, was shielded from environmental exposure during the LDEF flight and only exposed to

vacuum. During the EOIM-III test, both materials were exposed to 2.3×10^{20} oxygen atoms/cm^2.

SEM images of the surfaces of the two composite specimens are shown and 500X and 1000X magnifications in figures 16 and 17, respectively. The specimen exposed only to space vacuum during the LDEF flight eroded much faster than the LEO exposed specimen, as indicated by the quantity of carbon fiber revealed.

ESCA analyses revealed the reason for the AO erosion behavior. The LEO exposed LDEF specimen had approximately 25 atomic % silicon on its surface, before or after EOIM-III exposure. The composite specimen exposed only to vacuum during the LDEF flight had approximately 2.2 atomic % silicon on its surface. The test objective, to determine the effect of previous solar exposure on AO erosion rate, was not accomplished. However, silicon contamination from previous exposure was observed to provide some protection against AO erosion.

Ag/FEP

Specimens of Ag/FEP thermal blanket material from LDEF experiment A0178 were taken from trailing edge locations. This material had been subjected to between about 8200 and 9600 equivalent sun hours of solar ultraviolet radiation and about 33,000 thermal cycles. One specimen was taken from the edge of a blanket and had been subjected to less solar exposure. Particular specimens were then selected from this set of specimens and flown on EOIM III to provide atomic oxygen exposure to this material. The goal was to determine if the prior UV exposure would cause the material to degrade at a faster rate than new specimens. Surface contamination, deposited during the shuttle flight and remaining from the LDEF flight, masked any such effect.

The specimens were each characterized by surface analysis using ESCA. Table 2 shows the results of this examination. The relative CF and CF_3 peak intensities compared to the CF_2 peak intensity, were determined before and after the EOIM III flight and for ground control material. Significant relative increases in the CF and CF_3 peak intensities were observed for all flight specimens in comparison with the ground control material. The specimen from the edge of B-5 which is listed as "shielded" from solar UV was actually exposed to some direct and some reflected solar UV. Carbon 1s ESCA spectra of the pre-EOIM III flight F-2 specimens show substantial contamination on the LDEF specimen. The post-EOIM III F-2 flight specimen shows that the level of atomic oxygen exposure on EOIM III removed substantial contamination from the previously flown material.

The CF_3/CF_2 carbon 1s peak intensity ratio is lower for each LDEF specimen reflown on EOIM III in comparison with each corresponding LDEF specimen (taken from the same blanket) not reflown. This indicates the oxygen is removing some of the surface FEP material previously altered by solar exposure. Figures 18 and 19 show the comparison between surface conditions on blanket F2 after the LDEF flight and after the subsequent EOIM III flight.

Table 2. Ag/FEP ESCA measurements showing CF and CF_3 relative to CF_2 peak intensities with environmental exposure.

Specimens	Peak Intensities		Exposures	
	CF	CF_3	UV(Hrs)	AO(Atoms/cm^2)
Ground control Specimens				
	0.045	0.07		
LDEF Specimens				
B-5	0.45	0.67	8200	$9.6x10^{12}$
C-5	0.46	0.65	8200	$1.5x10^{17}$
F-2	0.87, 1.06	0.40, 0.50	9600	$1.5x10^{17}$
E-2	0.47, 0.69	0.90, 0.73	9600	$1.5x10^{17}$
LDEF Specimens reflown on EOIM-III				
B-5	1.0, 0.89	0.18, 0.19	8200	$2.3x10^{20}$
B-5(Shielded)	0.94, 0.88	0.15, 0.25	-	$2.3x10^{20}$
F-2	0.89, 1.0	0.17, 0.20	9600	$2.3x10^{20}$

Polyurethane Thermal Control Paint Chemglaze A276

Four specimens of white polyurethane thermal control coating, Chemglaze A276, were taken from LDEF tray clamps (ref. 3). Two of these specimens were flown on EOIM-III. The other two specimens were used as ground control specimens to monitor any non-flight induced changes. The environmental conditions of exposure and the optical properties of the coating surfaces before and after EOIM-III flight are shown in Table 3 for both the flight and ground control specimens. The visual appearance of the A276 specimens is shown in figure 20. As expected, the AO erosion from the EOIM-III flight was sufficient to remove much of the solar ultraviolet (UV) radiation-damaged polyurethane resin in the paint surface, exposing white pigment and recovering some of the reflectivity exhibited by the control.

Table 3. Pre- and Postflight Exposure and Optical Properties for LDEF Chemglaze A276 Coating Specimens Flown on EOIM-III.

	EOIM-III Preflight				EOIM-III Postflight			
Sample	UV (ESH)	AO (atoms/cm2)	α_s	ε	UV (ESH)	AO (atoms/cm2)	α_s	ε
F1-6	8500	1.5x10E17	0.52	0.86	8500	2.3x10E20	0.35	0.88
D6-1	7100	7.3x10E16	0.48	0.88	7100	2.3x10E20	0.30	0.90
C5-2	9400	6.8x10E8	0.53	0.86	Not Flown		0.52	0.86
B2-4	9600	1.5x10E17	0.54	0.87	Not Flown		0.52	0.87
Control	-	-	0.28	0.87	Not Flown			

An interesting comparison can be made between the EOIM-III flight specimens and LDEF data for A276, plotting solar absorptance as a function of atomic oxygen fluence, shown in figure 21. The EOIM-III specimens, after sequential exposure to UV radiation then AO, follow the trend observed for LDEF specimens. The UV damaged portion of the polyurethane paint is the extreme surface of the resin fraction, and AO erosion of the surface resin provided some recovery of the coating's solar absorptance. AO erosion also increased thermal emissivity slightly.

SUMMARY

The significance of the EOIM-III flight for the materials investigated here was that short-term atomic oxygen exposure did produce some observable effects. However, the usefulness of short-term exposure can be significantly limited by contamination. Contamination on the graphite/epoxy composites of this investigation essentially precluded the intended evaluation of UV radiation effects on AO erosion rates. Regardless of contamination effects, the exposure levels on STS-046 provide only an indication of the changes in materials caused by the LEO space environment. Long-term exposure or accelerated exposure techniques are needed to provide more confidence in materials performance life predictions with space environmental exposure.

ACKNOWLEDGEMENTS

Appreciation is extended NASA for the opportunity to conduct valuable experiments such as EOIM-III. A special thanks is extended to Shirley Chung of JPL and Miria Finckenor of MSFC for their extensive efforts in the integration and de-integration analyses of the materials discussed herein.

REFERENCES

1. S. Y. Chung, D. E. Brinza, A. E. Stiegman, J. T. Kenny, and R. H. Liang, Flight- and Ground-Test Correlation Study of BMDO SDS Materials: Phase I Report, JPL Publication 93-31, December 1993.

2. C. R. Maag, D. E. Williams, E. N. Borson, J. J. Palou, Induced Payload Contamination as Observed on Three Successive Flights of the Space Shuttle. Third LDEF Post-Retrieval Symposium.

3. J. L. Golden: Results of Examination of the A276 White and Z306 Black Thermal Control Paint Disks Flown on LDEF. First LDEF Post-Retrieval Symposium, NASA CP-3134, Vol. 2, p. 975, 1992.

ANALYSIS OF SELECTED SPECIMENS FROM THE STS-46 ENERGETIC OXYGEN INTERACTION WITH MATERIALS-III EXPERIMENT

Johnny L. Golden, Roger J. Bourassa, Harry W. Dursch and H. Gary Pippin

Boeing Defense & Space Group
P.O. Box 3999 M/S 82-32
Seattle, WA 98124-2499
(206) 773-2846, FAX (206) 773-4946

INTRODUCTION

The Energetic Oxygen Interaction with Materials III (EOIM-III) experiment was flown on the STS-46 mission, which was launched on July 31, 1992 and returned August 8,

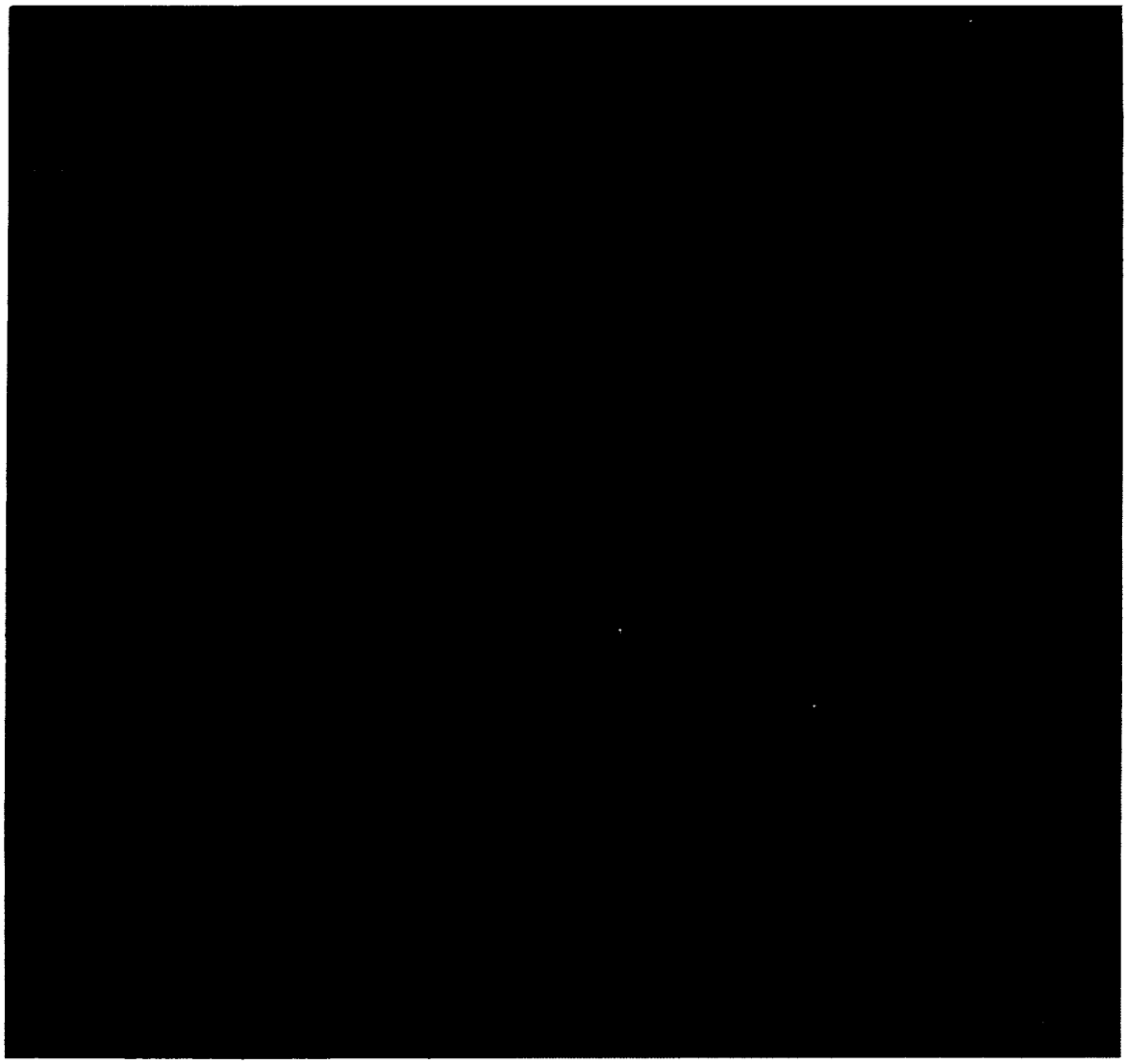

Figure 1. EOIM-III postflight view of solid film lubricant Torlon 4301.

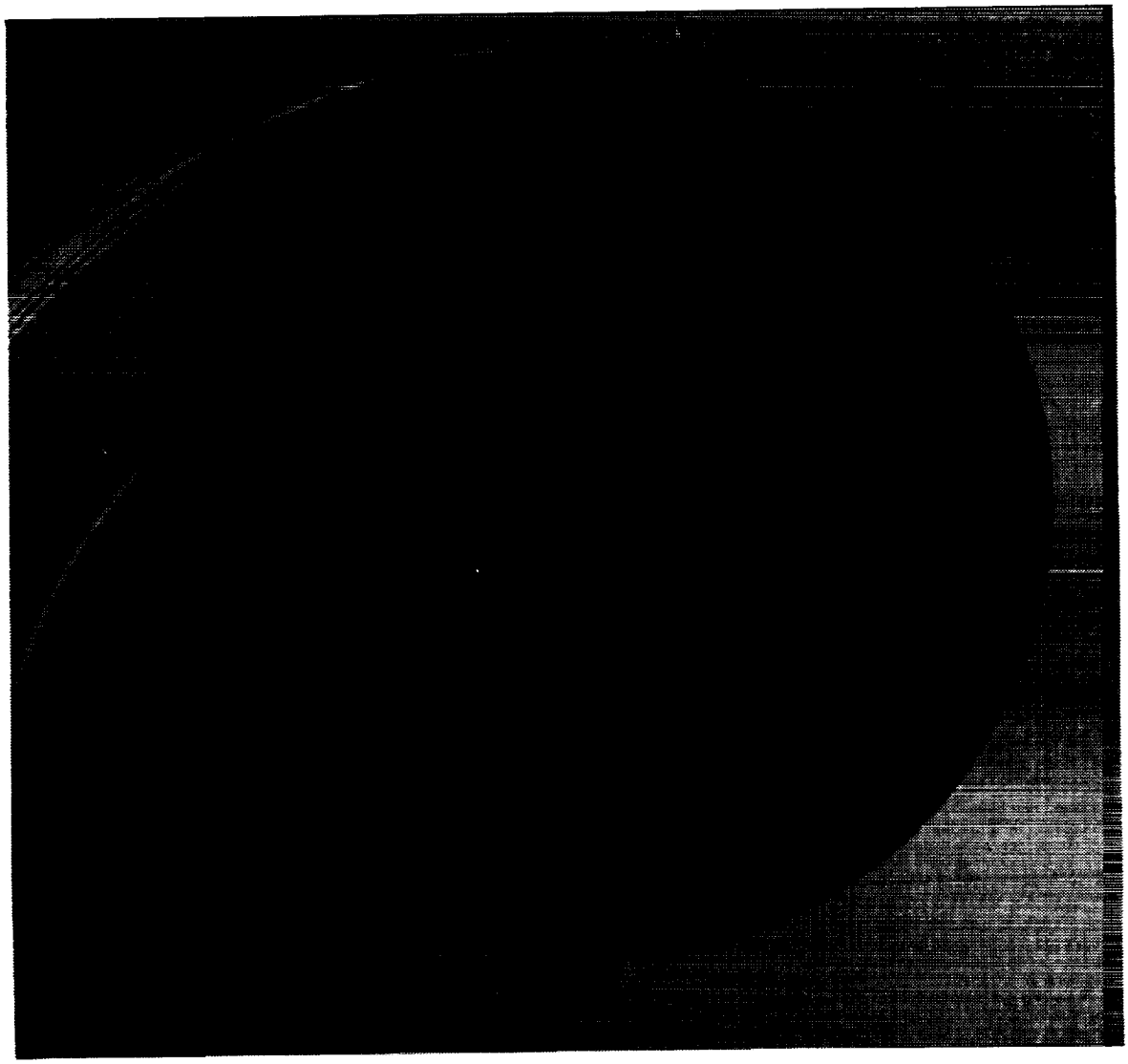

Figure 2. EOIM-III postflight view of solid film lubricant Delrin 100AF.

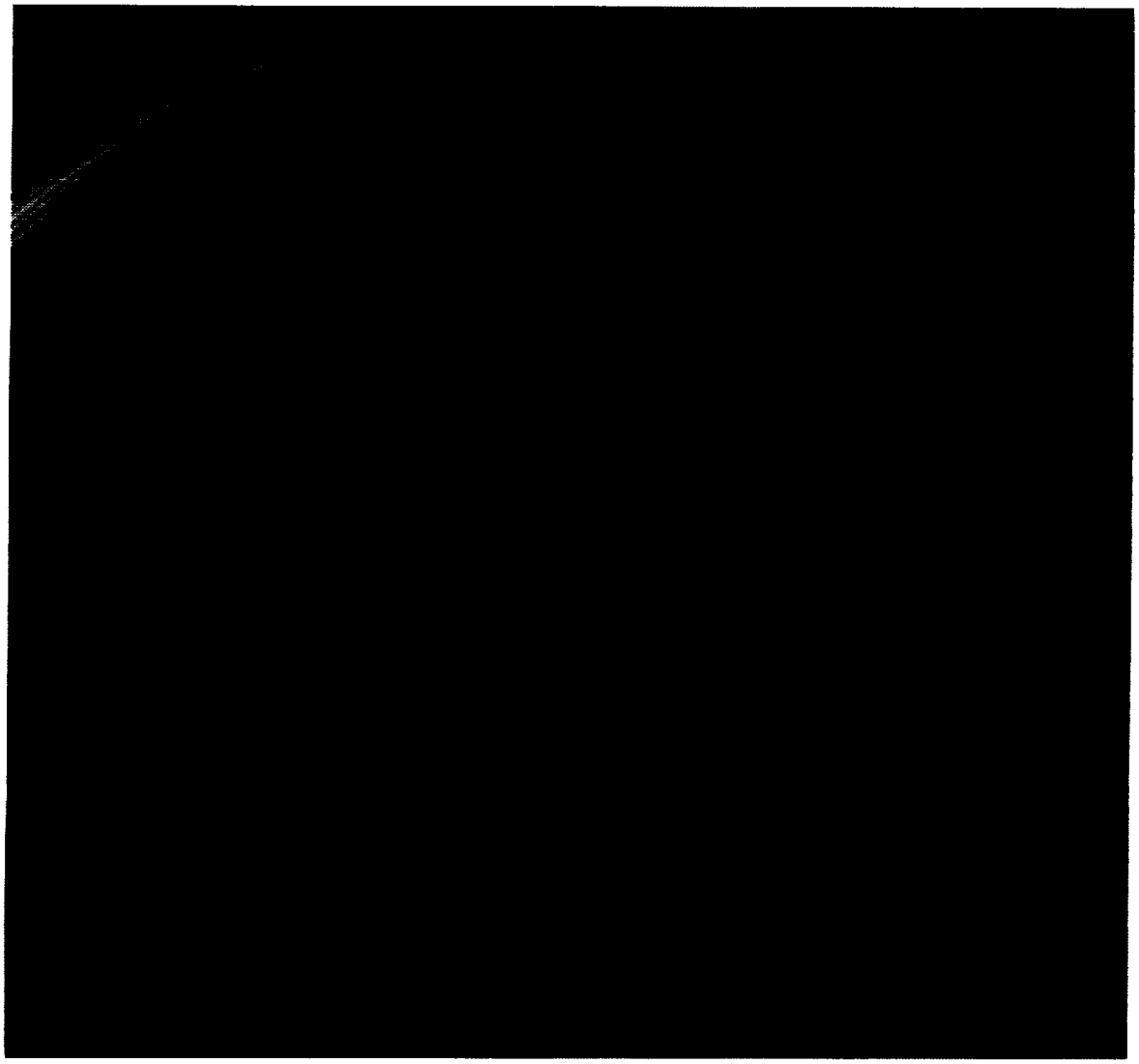

Figure 3. EOIM-III postflight view of solid film lubricant PS212.

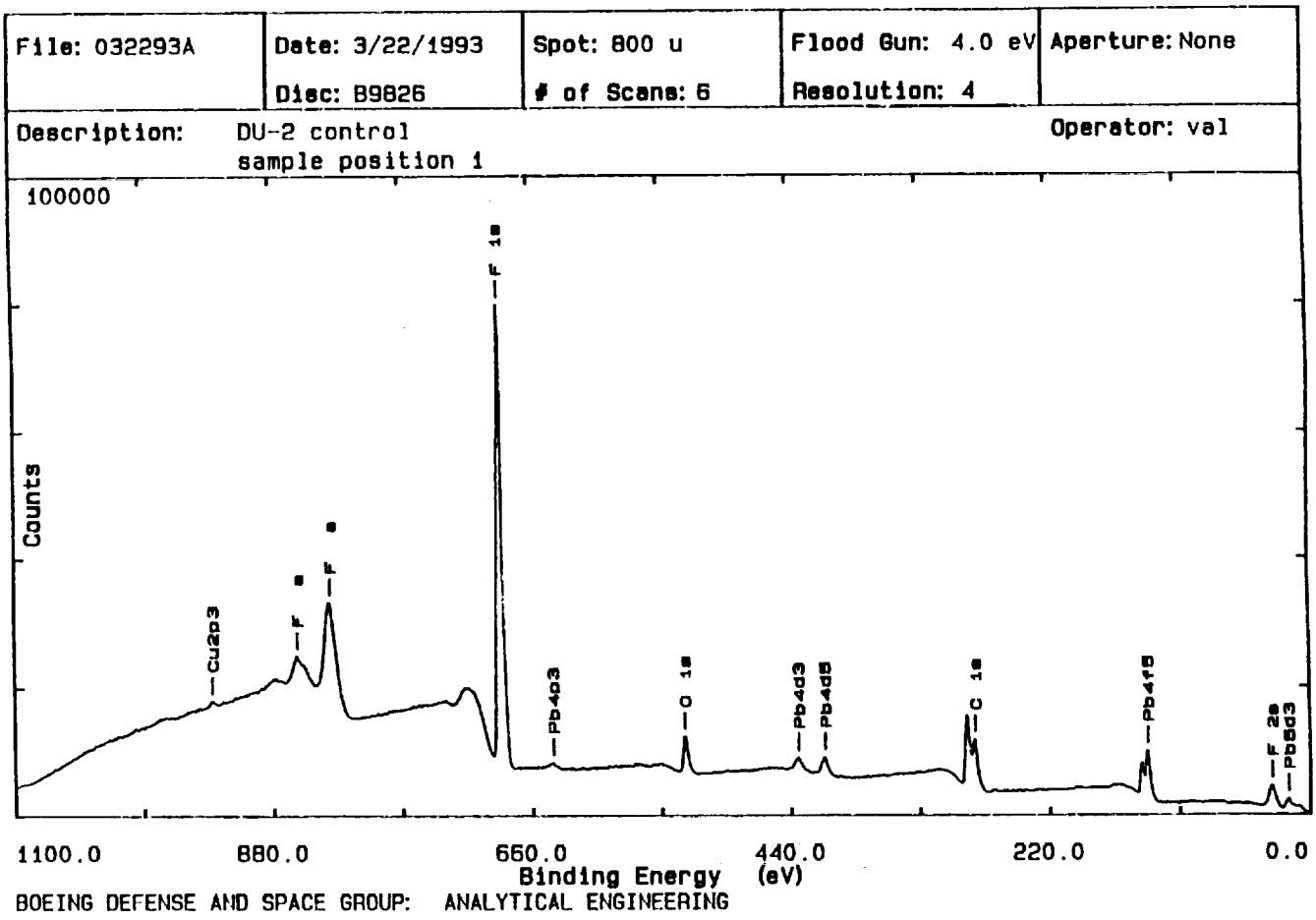

Figure 4. X-ray photoelectron spectroscopy of solid film lubricant Garlock DU control specimen.

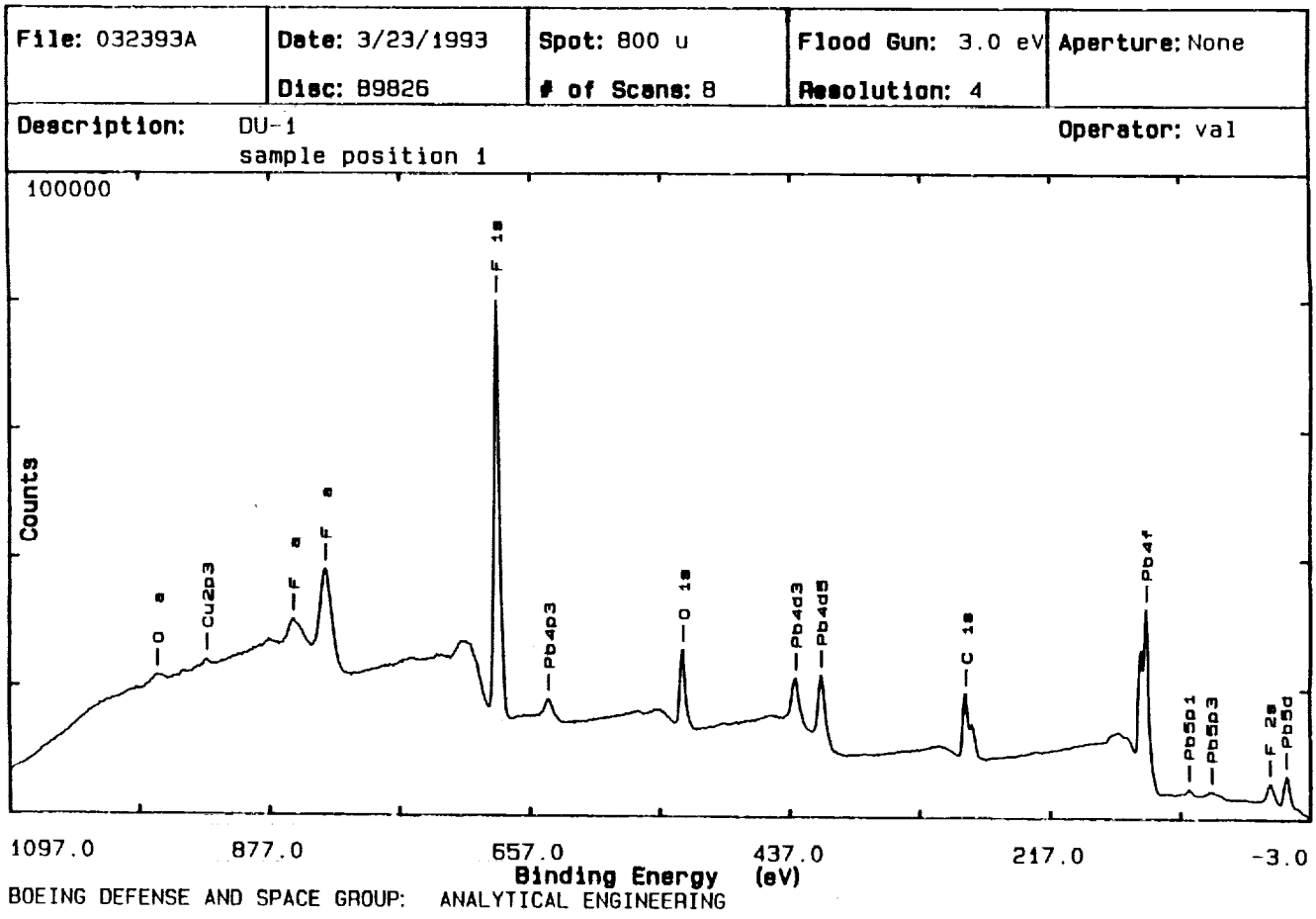

Figure 5. X-ray photoelectron spectroscopy of solid film lubricant Garlock DU flight specimen.

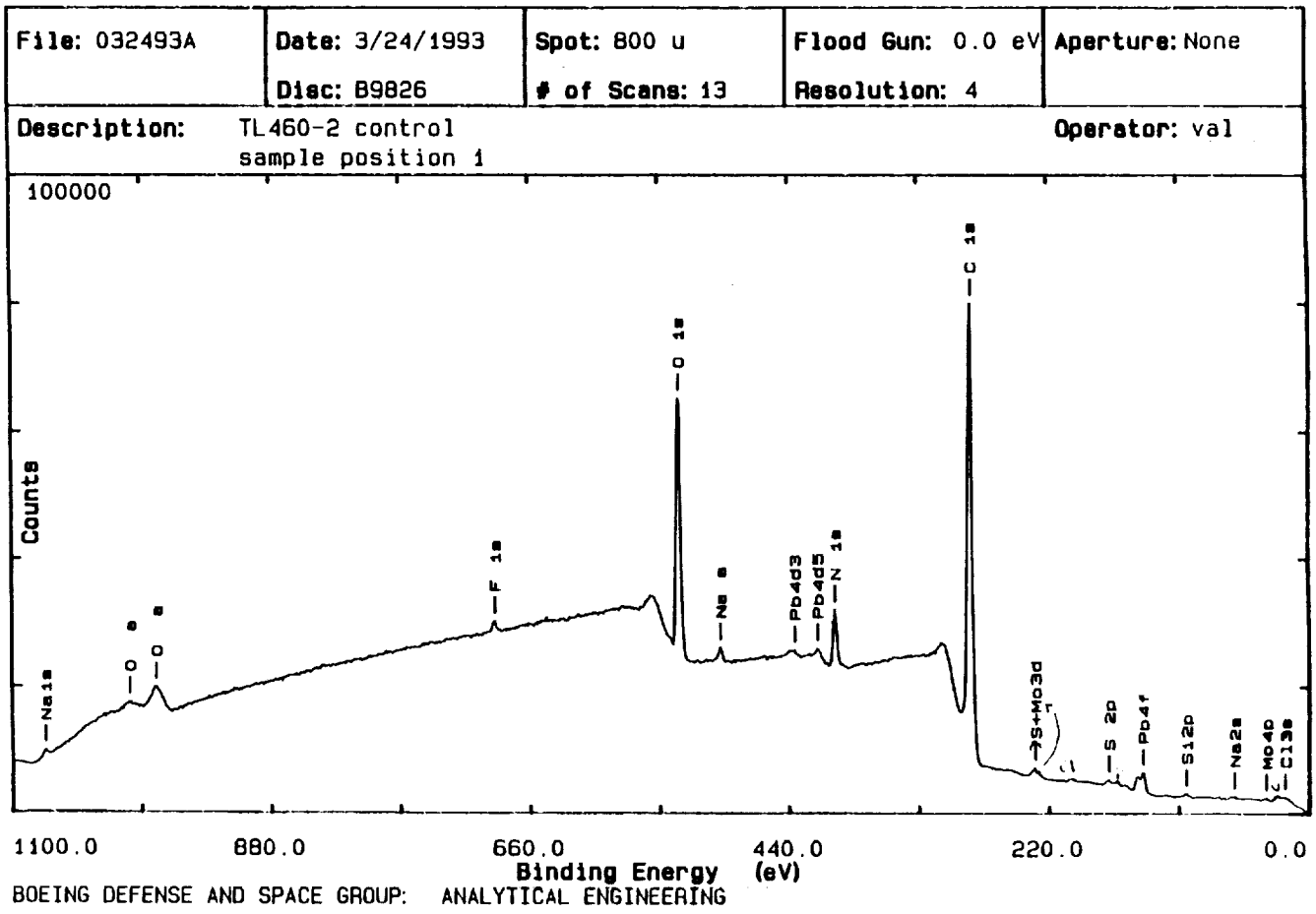

Figure 6. X-ray photoelectron spectroscopy of solid film lubricant Tiolube 460 control specimen.

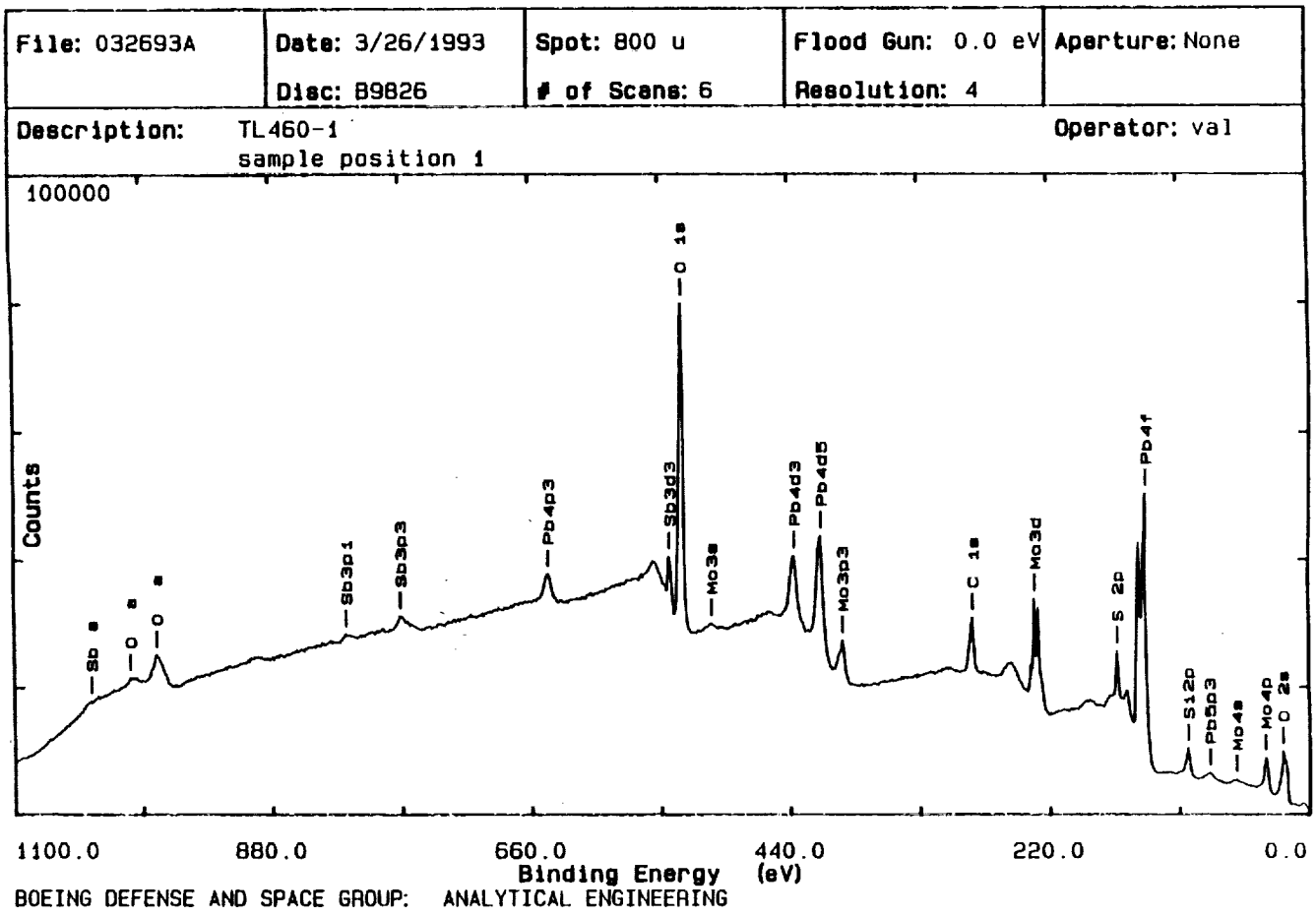

Figure 7. X-ray photoelectron spectroscopy of solid film lubricant Tiolube 460 flight specimen.

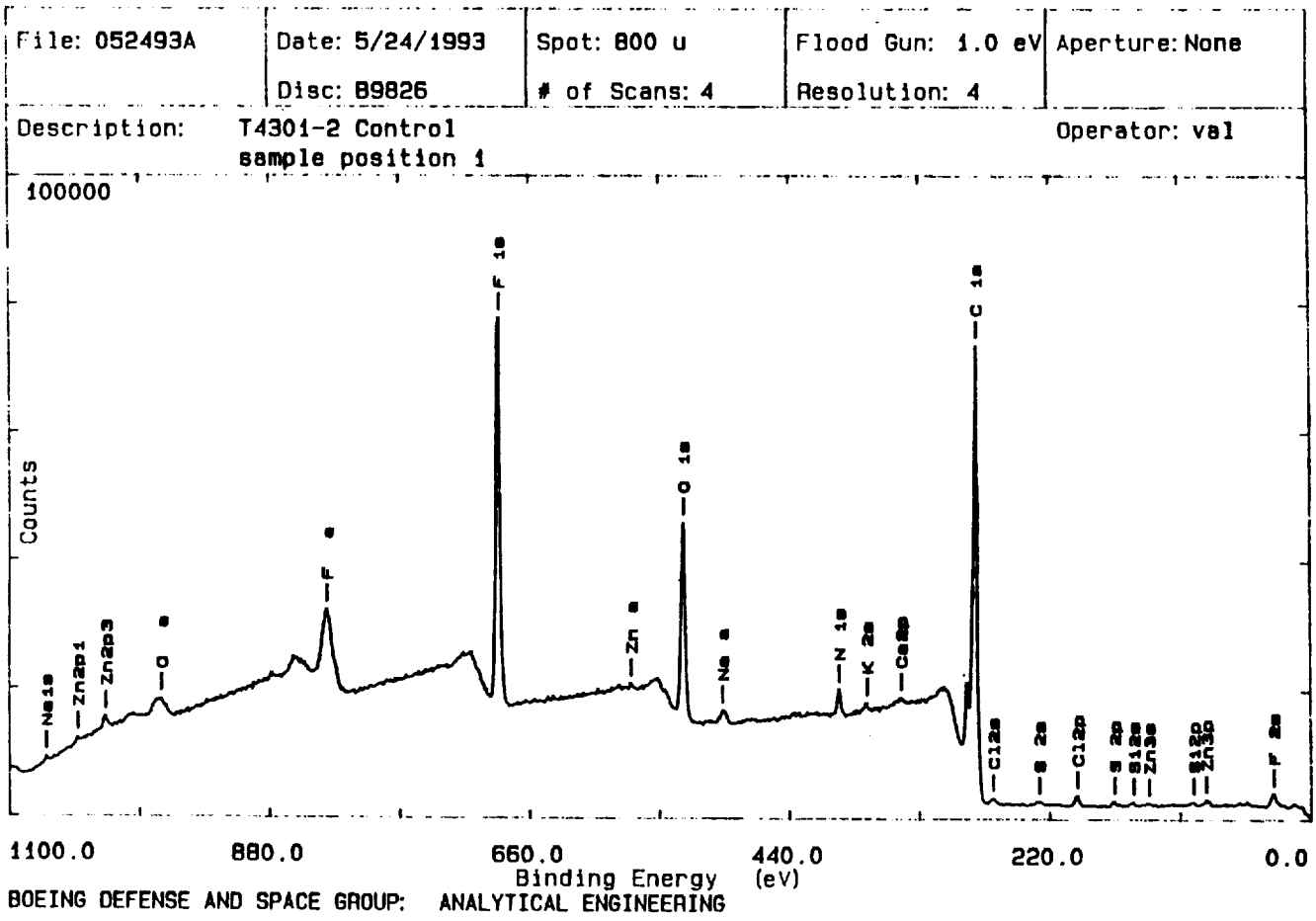

Figure 8. X-ray photoelectron spectroscopy of solid film lubricant Torlon 4301 control specimen.

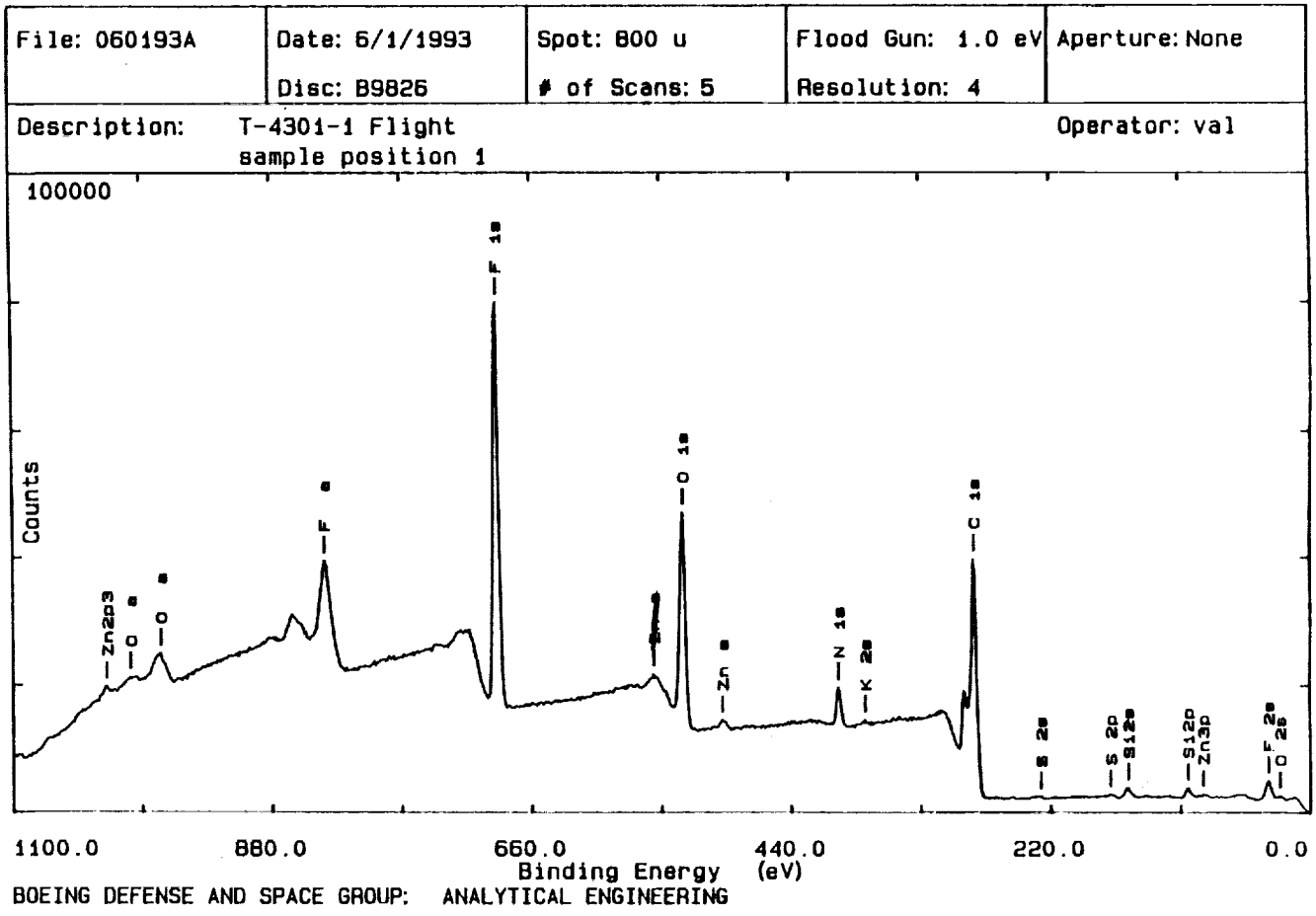

Figure 9. X-ray photoelectron spectroscopy of solid film lubricant Torlon 4301 flight specimen.

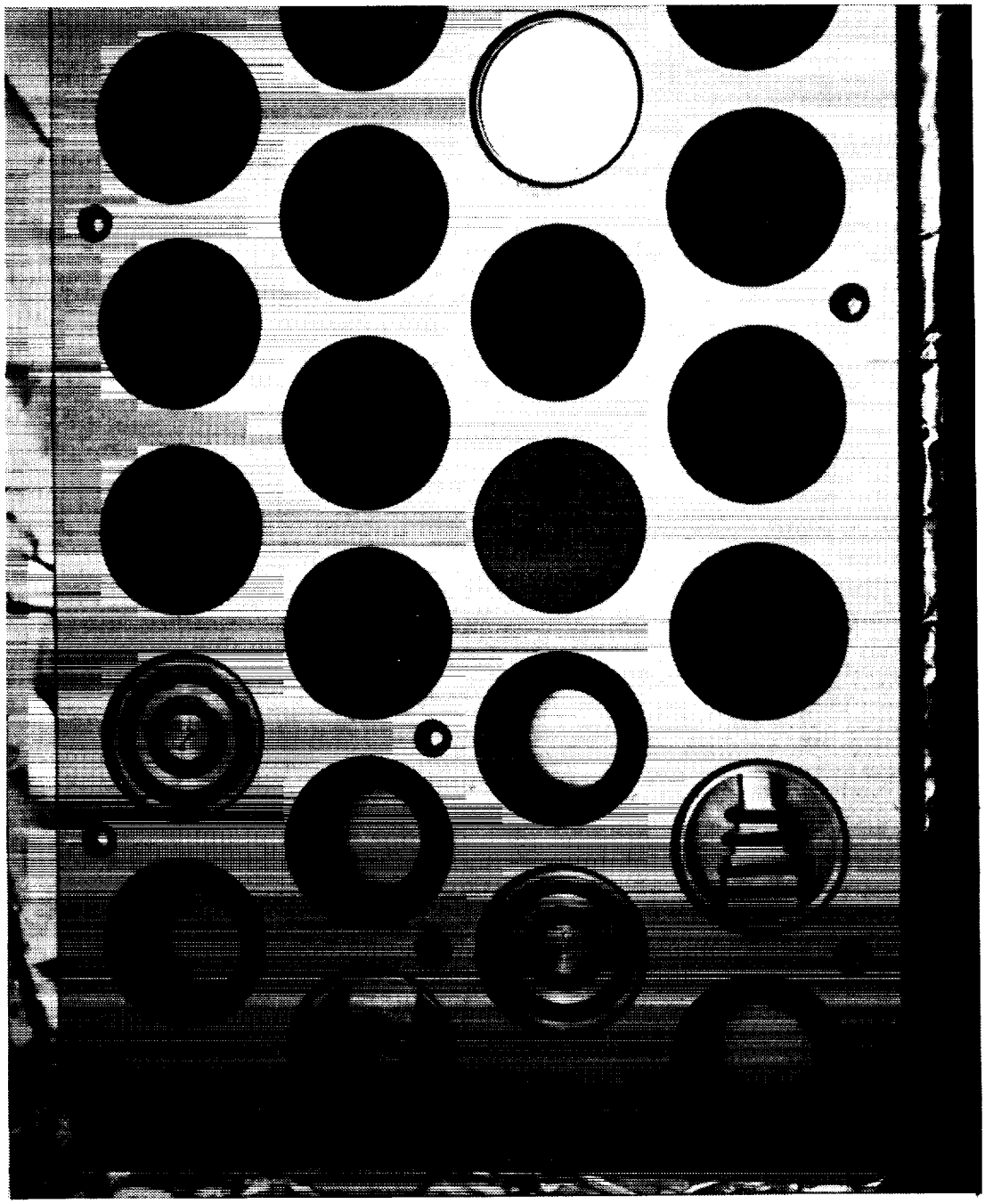

Figure 10. EOIM-III preflight view of the tensile and compressive o-ring fixtures in the experiment tray.

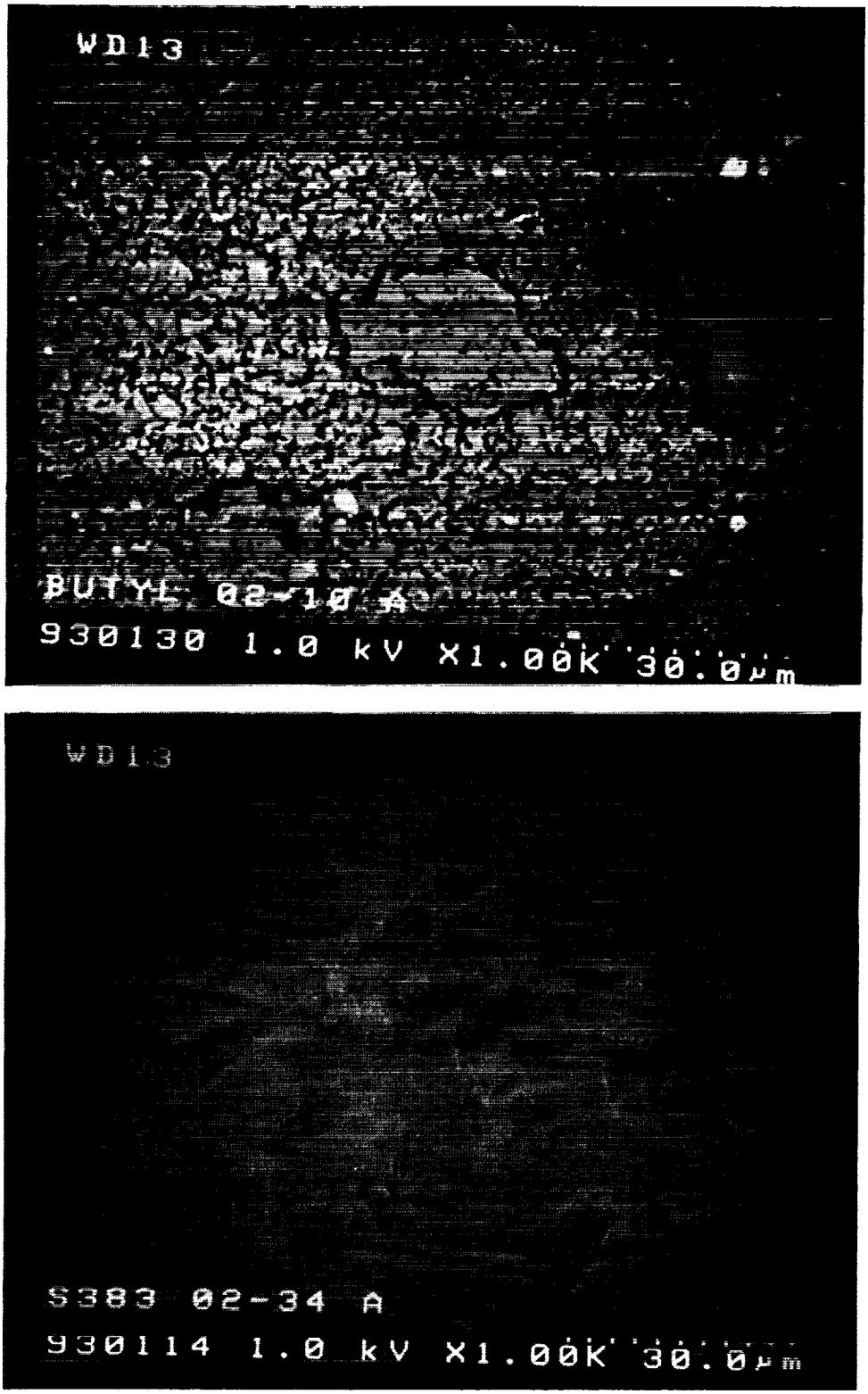

Figure 11. Scanning electron microscope images of o-rings postflight at 1000X magnification. The images are of specimens flown under compression. The top image is of a butyl rubber specimen, the bottom image is of a silicone (S383).

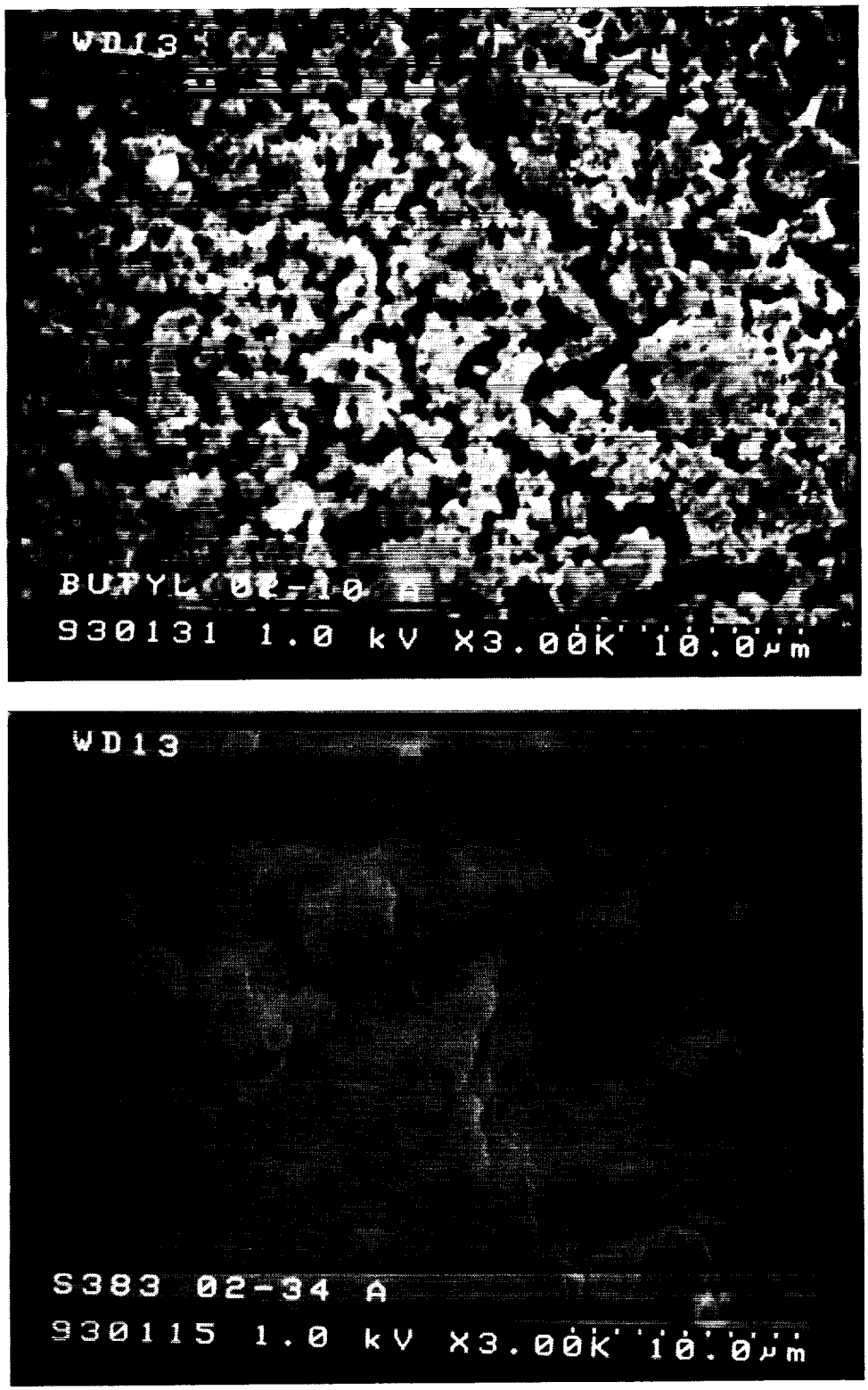

Figure 12. Scanning electron microscope images of o-rings postflight at 3000X magnification. The images are of specimens flown under compression. The top image is of a butyl rubber specimen, the bottom image is of a silicone (S383).

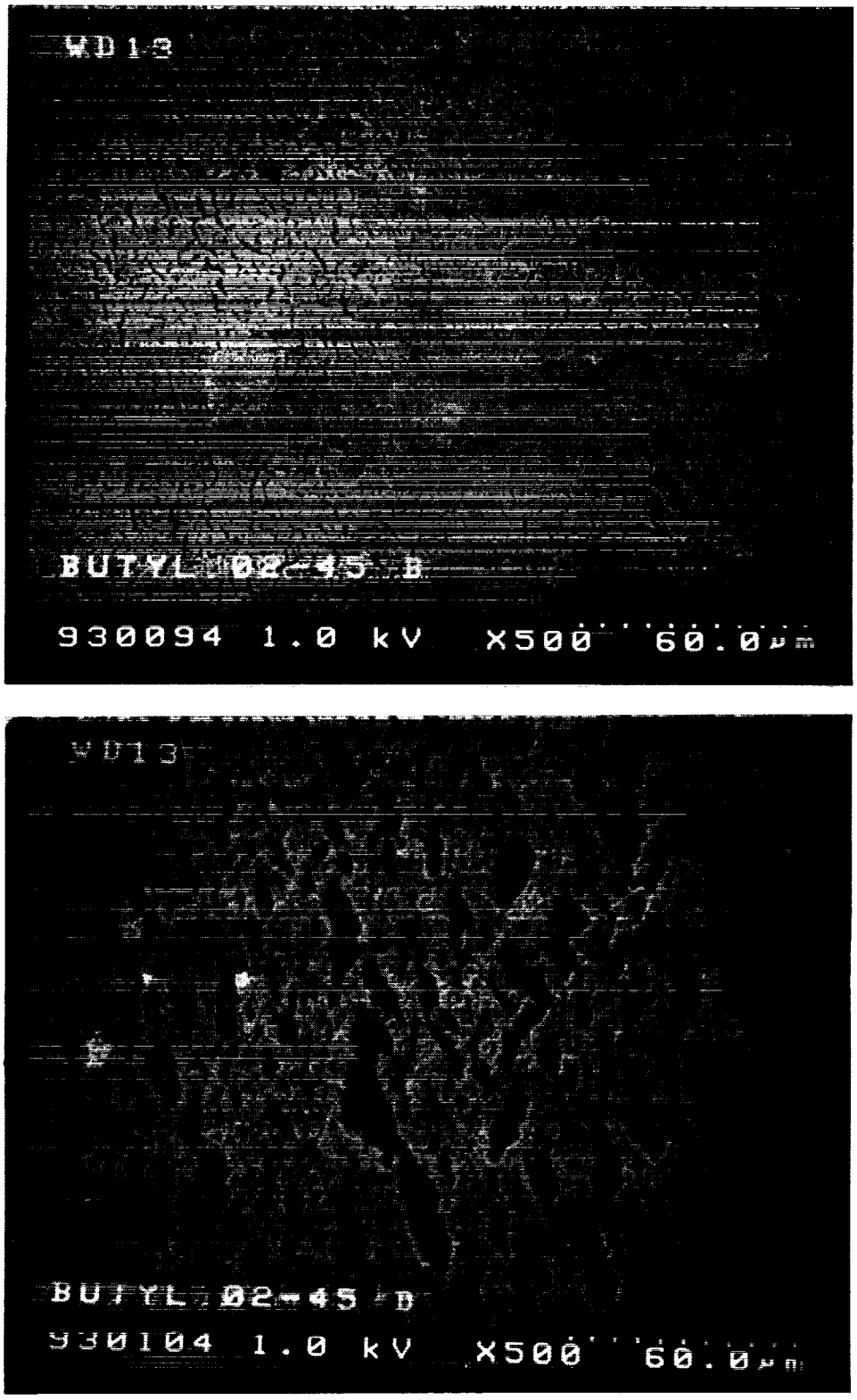

Figure 13. Scanning electron microscope images of butyl rubber o-rings postflight at 500X magnification, showing the effect of tension on atomic oxygen erosion. The top image is of a specimen flown under 60% tension. The bottom image is of a specimen flown under 100% tension.

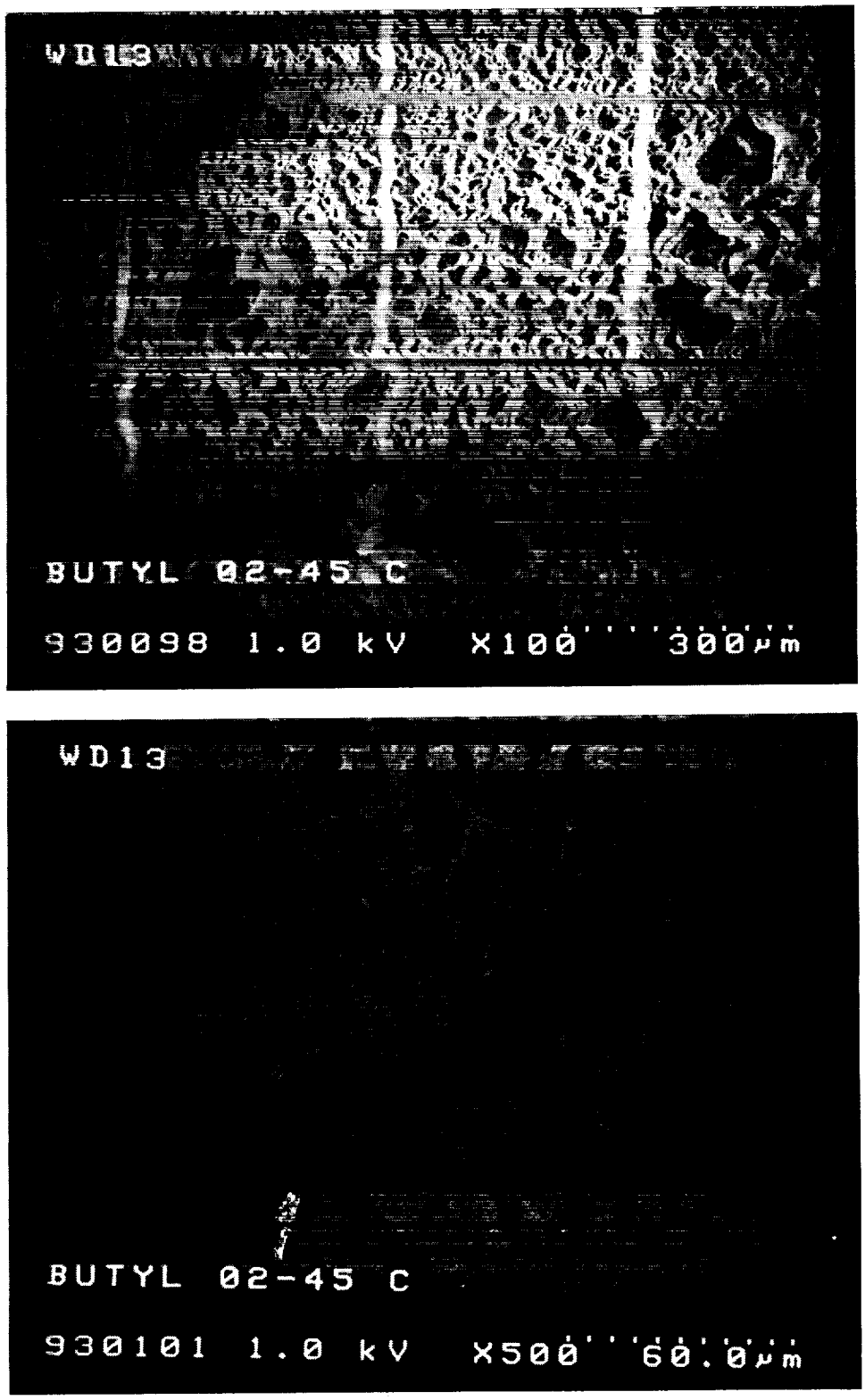

Figure 14. Scanning electron microscope images of a butyl rubber o-ring postflight at 100X and 500X magnification. This o-ring was flown under 80% tension.

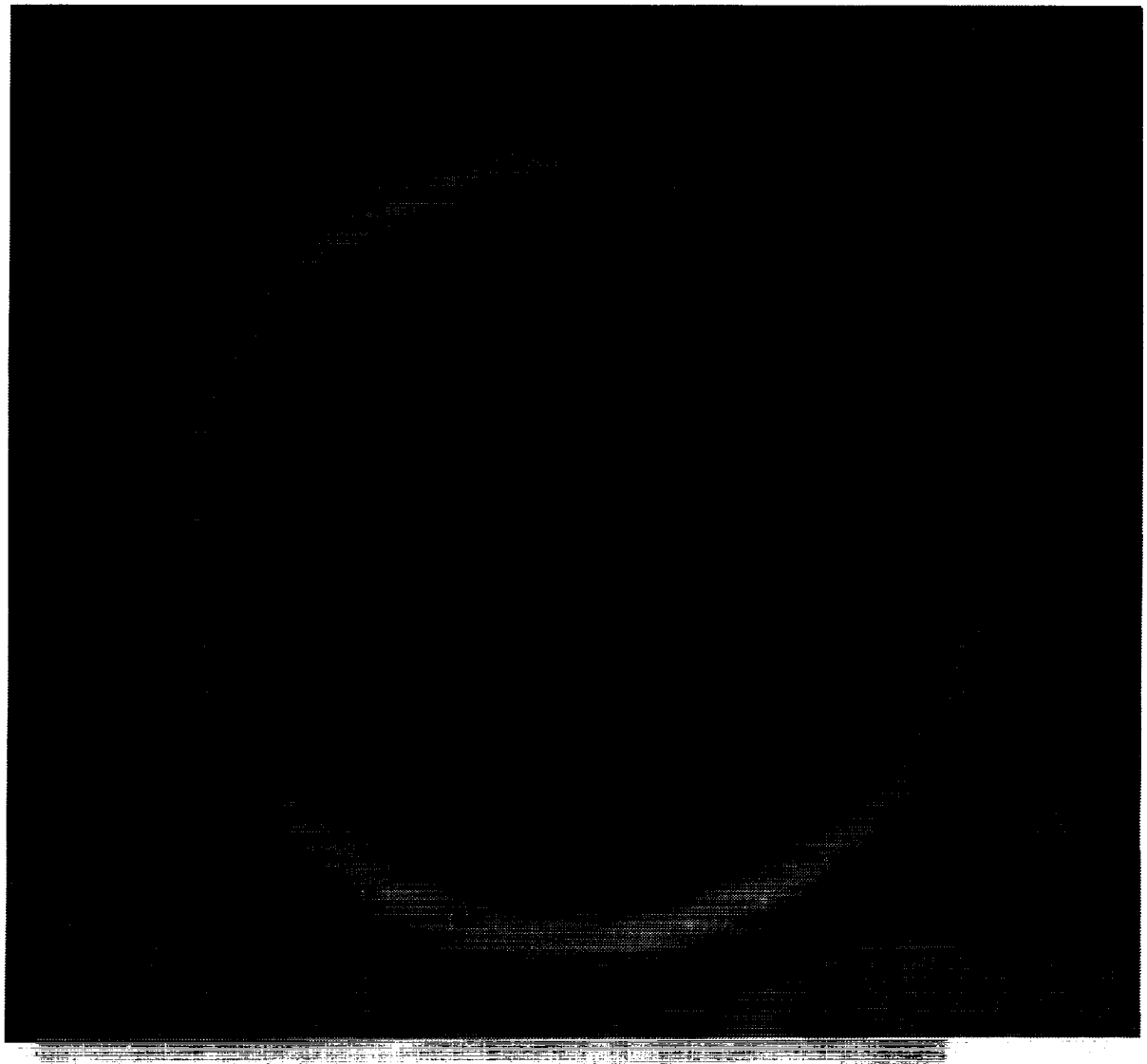

Figure 15. Fluorescence behavior of the silicone rubber o-ring postflight.

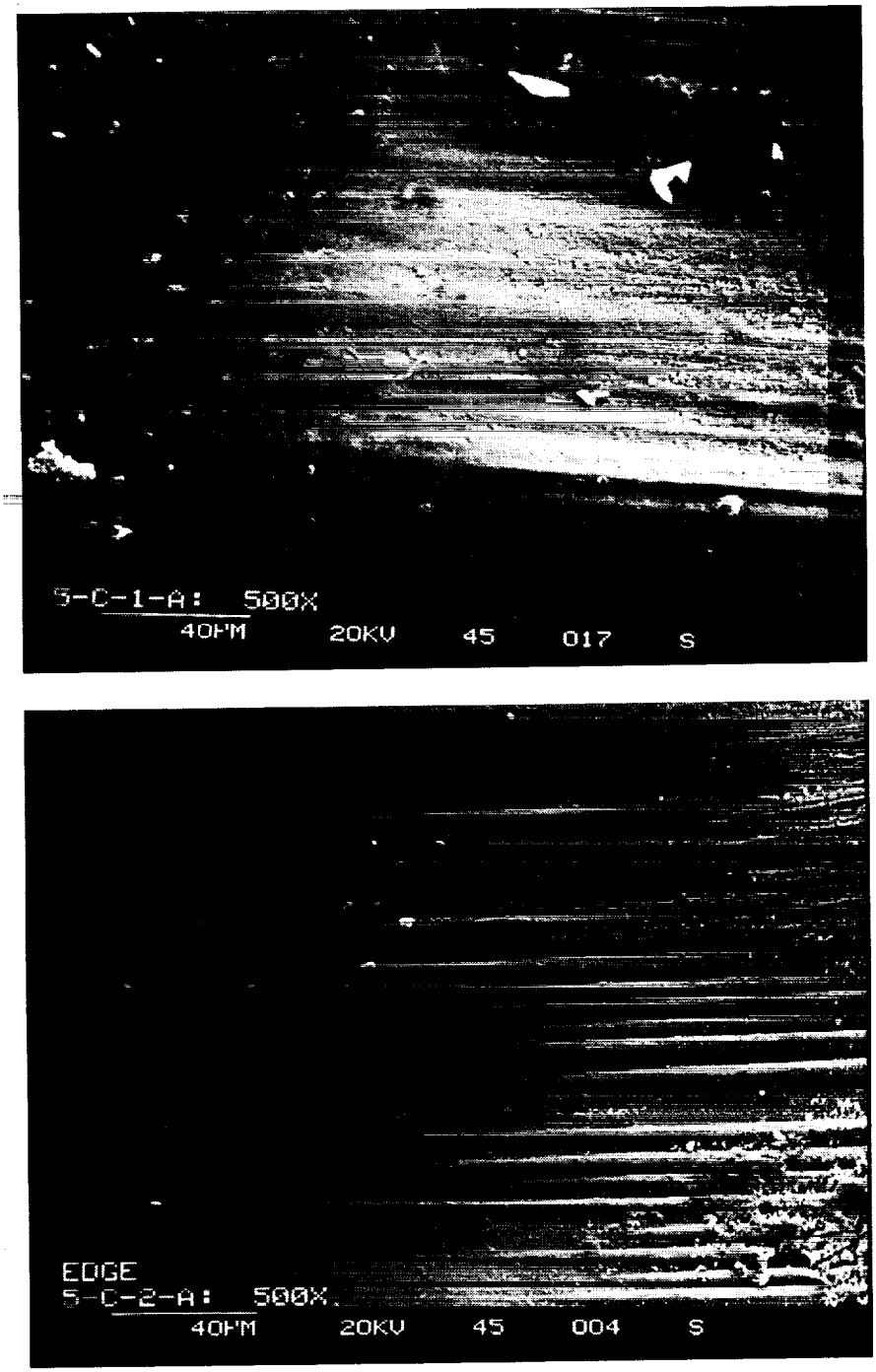

Figure 16. Scanning electron microscope images of two graphite/epoxy composite specimens at 500X magnification. The specimens were each flown on LDEF and then the EOIM-III experiment. The top image is of a specimen directly exposed to space on LDEF. The bottom image is of a specimen shielded by other specimens on LDEF.

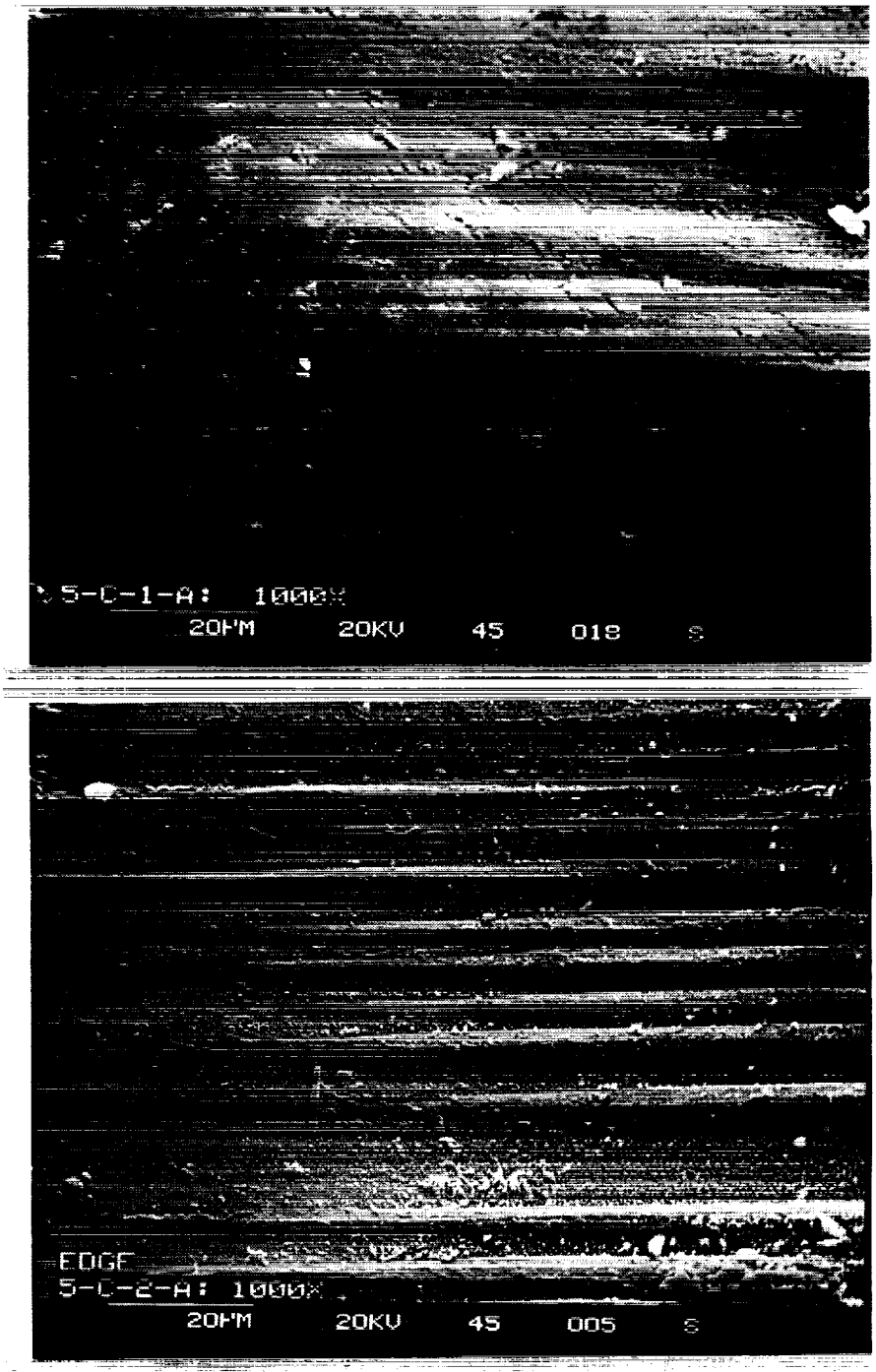

Figure 17. Scanning electron microscope images of two graphite/epoxy composite specimens at 1000X magnification. The specimens were each flown on LDEF and then the EOIM-III experiment. The top image is of a specimen directly exposed to space on LDEF. The bottom image is of a specimen shielded by other specimens on LDEF.

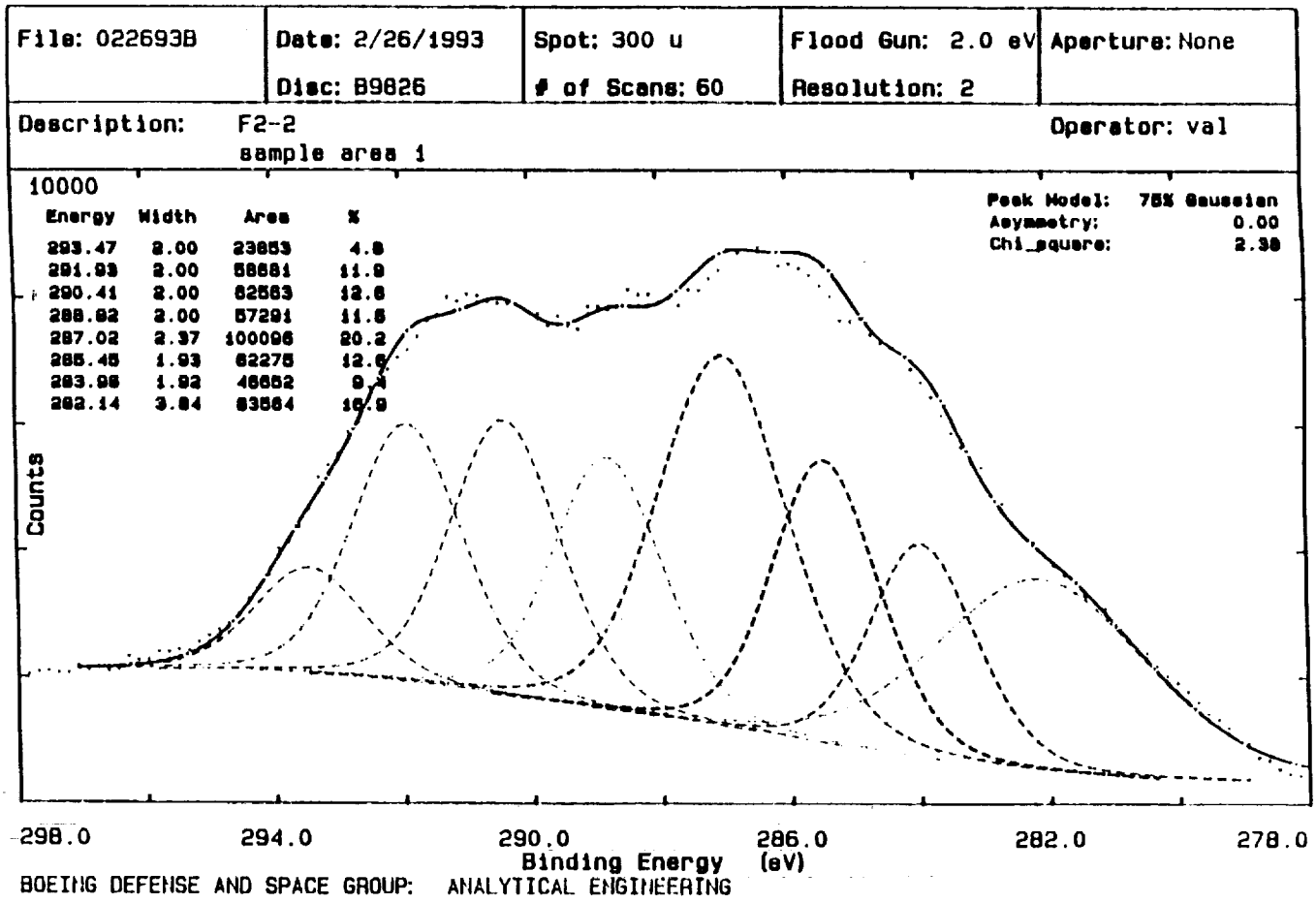

Figure 18. ESCA measurement of Ag/FEP specimen from LDEF tray F2, analyzing the carbon 1s binding energy region.

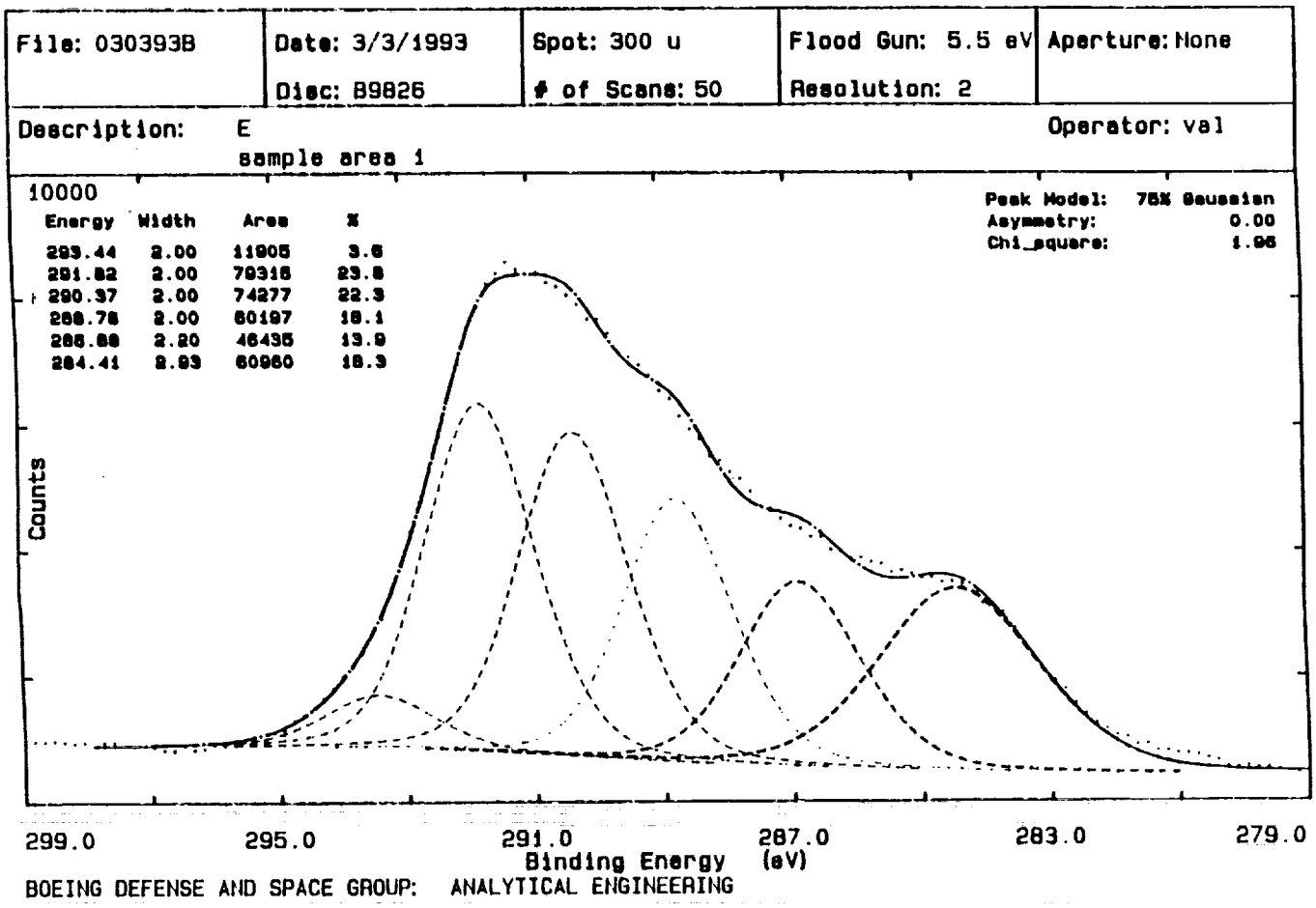

Figure 19. ESCA measurement of Ag/FEP specimen from LDEF tray F2, reflown on EOIM III, analyzing the carbon 1s binding energy region.

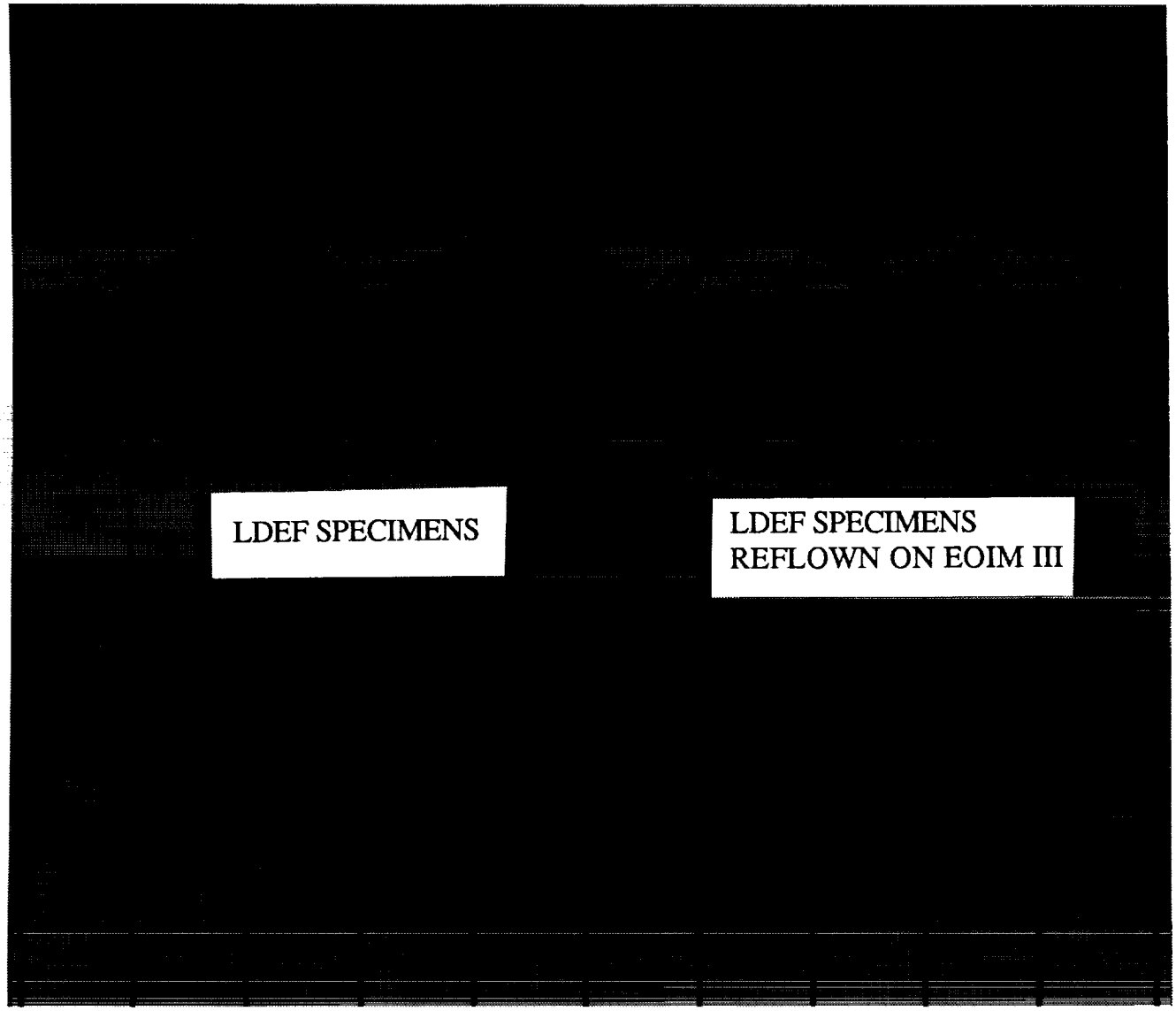

Figure 20. Chemglaze A276 polyurethane paint specimens previously flown on LDEF, shown with and without environmental exposure on EOIM-III.

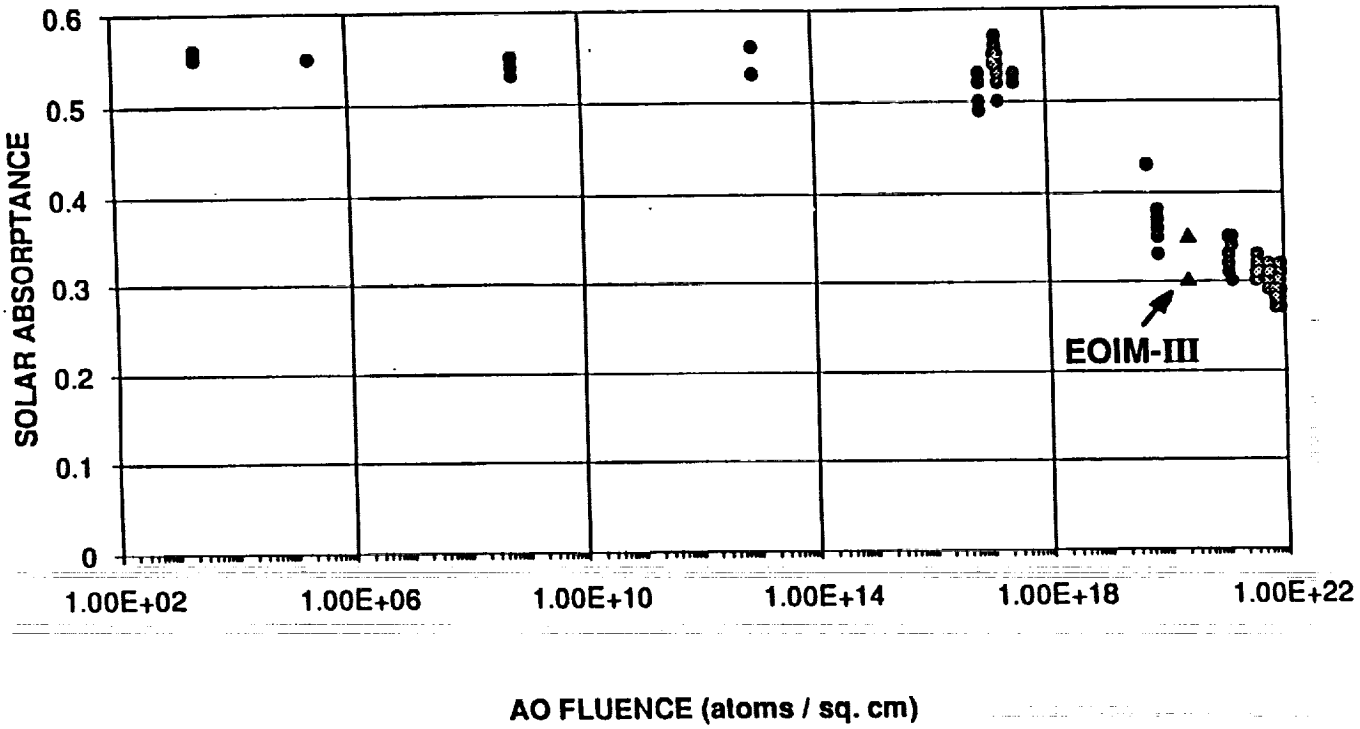

Figure 21. Comparison of solar absorptance results for EOIM-III specimens of Chemglaze A276 to those obtained for overall LDEF mission, as a function of atomic oxygen fluence. The LDEF data is shown by the filled circles and the EOIM-III data is shown by the filled triangles.